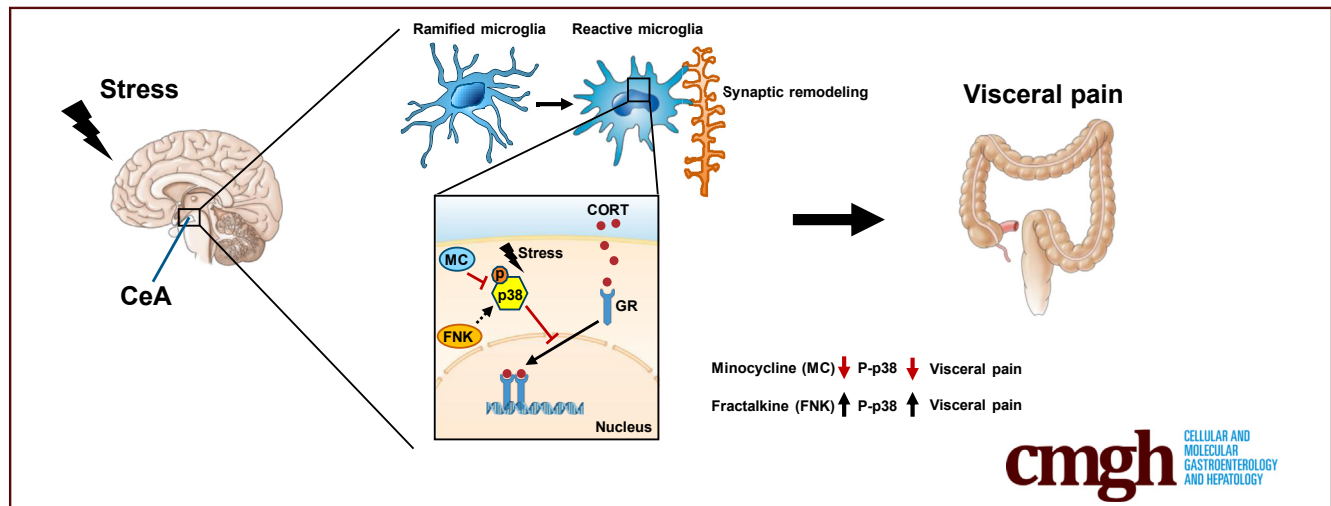


ORIGINAL RESEARCH

Inhibition of Microglial Activation in the Amygdala Reverses Stress-Induced Abdominal Pain in the Male Rat

Tian Yuan,¹ Krishna Manohar,¹ Rocco Latorre,⁴ Albert Oroch,¹ and Beverley Greenwood-Van Meerveld^{1,2,3}¹Oklahoma Center for Neuroscience, University of Oklahoma Health Sciences Center, Oklahoma City, Oklahoma; ³Department of Physiology, University of Oklahoma Health Sciences Center, Oklahoma City, Oklahoma; ²Oklahoma City VA Health Care System, Oklahoma City, Oklahoma; and ⁴Department of Basic Science and Craniofacial Biology, New York University, New York City, New York

SUMMARY

Microglial remodeling in the central nucleus of the amygdala contributes to chronic stress-induced visceral hypersensitivity via microglial p38 mitogen-activated protein kinase activation, glucocorticoid receptor dysfunction, and synaptic plasticity. Inhibition of microglial activity in the central nucleus of the amygdala is sufficient to attenuate stress-induced visceral hypersensitivity.

BACKGROUND & AIMS: Psychological stress is a trigger for the development of irritable bowel syndrome and associated symptoms including abdominal pain. Although irritable bowel syndrome patients show increased activation in the limbic brain, including the amygdala, the underlying molecular and cellular mechanisms regulating visceral nociception in the central nervous system are incompletely understood. In a rodent model of chronic stress, we explored the role of microglia in the central nucleus of the amygdala (CeA) in controlling visceral sensitivity. Microglia are activated by environmental challenges such as stress, and are able to modify neuronal activity via synaptic remodeling and inflammatory cytokine release. Inflammatory gene expression and microglial activity are regulated negatively by nuclear glucocorticoid receptors (GR), which are suppressed by the stress-activated pain mediator p38 mitogen-activated protein kinases (MAPK).

METHODS: Fisher-344 male rats were exposed to water avoidance stress (WAS) for 1 hour per day for 7 days. Microglia morphology and the expression of phospho-p38 MAPK and GR were analyzed via immunofluorescence. Microglia-mediated synaptic remodeling was investigated by quantifying the number of postsynaptic density protein 95-positive puncta. Cytokine expression levels in the CeA were assessed via quantitative polymerase chain reaction and a Luminex assay (Bio-Rad, Hercules, CA). Stereotaxic infusion into the CeA of minocycline to inhibit, or fractalkine to activate, microglia was followed by colonic sensitivity measurement via a visceromotor behavioral response to isobaric graded pressures of tonic colorectal distension.

RESULTS: WAS induced microglial deramification in the CeA. Moreover, WAS induced a 3-fold increase in the expression of phospho-p38 and decreased the ratio of nuclear GR in the microglia. The number of microglia-engulfed postsynaptic density protein 95-positive puncta in the CeA was increased 3-fold by WAS, while cytokine levels were unchanged. WAS-induced changes in microglial morphology, microglia-mediated synaptic engulfment in the CeA, and visceral hypersensitivity were reversed by minocycline whereas in stress-naïve rats, fractalkine induced microglial deramification and visceral hypersensitivity.

CONCLUSIONS: Our data show that chronic stress induces visceral hypersensitivity in male rats and is associated with

microglial p38 MAPK activation, GR dysfunction, and neuronal remodeling in the CeA. (*Cell Mol Gastroenterol Hepatol* 2020;10:527–543; <https://doi.org/10.1016/j.jcmgh.2020.04.020>)

Keywords: IBS; Brain–Gut Axis; Chronic Psychological Stress; Visceral Hypersensitivity.

Irritable bowel syndrome (IBS) is a common and debilitating gastrointestinal disorder that is exacerbated by stress and characterized by abdominal pain and altered bowel movements in the absence of colonic mucosal damage.^{1,2} The component of the stress response mediated by the hypothalamic-pituitary-adrenal axis activates the adrenal cortex to release cortisol in human beings or corticosterone in rodents (CORT). During episodes of stress, CORT binds to glucocorticoid receptors (GRs) to modulate the stress response. In patients with IBS, several brain regions in the hypothalamic-pituitary-adrenal axis such as the amygdala, thalamus, and prefrontal cortex are associated with emotional arousal, endogenous pain modulation, and gastrointestinal hyperactivity.^{3–5} In support of these clinical observations, our previous research in experimental models has shown that the central nucleus of the amygdala (CeA) is an important structure for mediating visceral nociception in response to stress.^{6–8}

Microglia are considered the innate immune cells in the brain, and maintain central nervous system (CNS) homeostasis in response to changes in their microenvironment such as immune challenge and stress. Microglia are extremely plastic and microglial activation has been associated with specific morphologic changes; during activation, microglia retract their processes, resulting in decreased occupied area and increased soma size.⁹ Although microglia in the CNS have been implicated as an important mediator of the stress response,^{10,11} the role of microglia in the limbic brain, most notably the CeA, in the development stress-induced colonic hypersensitivity remains unknown. Therefore, the aim of the current study was to investigate whether chronic psychological stress modulates microglial plasticity in the CeA to drive a cascade of downstream cellular events that contribute to the development of stress-induced colonic allodynia and hyperalgesia. To address our experimental aim, we used a rodent model of water-avoidance stress (WAS), in which we and others have shown persistent colonic hypersensitivity to mechanical luminal distension.^{6,8,12,13} By using the WAS model, we investigated the effect of stress on the morphologic appearance of microglia in the CeA to determine whether a psychological stressor is capable of inducing microglial remodeling. We also aimed to determine whether exposure to stress alters the expression of p38 mitogen-activated protein kinase (p38 MAPK) signaling, which has been shown to mediate cellular responses to environmental stimuli and is associated with nociceptive processing.^{14–18} In addition, activated p38 MAPK directly inhibit GR nuclear translocation and its function by blocking its ligand binding site, leading to microglial structural and functional remodeling.^{19–21} Therefore, we measured GR subcellular expression within the CeA microglia after WAS. Because activated microglia can modify neuronal activity via synaptic remodeling and release of

inflammatory cytokines, we also quantified the microglia-mediated synaptic engulfment in rats subjected to chronic WAS, and assessed cytokine expression levels in the CeA. Finally, we hypothesized that pharmacologic modulation of microglial activity within the CeA would modulate colonic sensitivity. Therefore, we microinjected either minocycline to inhibit or fractalkine to activate microglia into the CeA stereotaxically, and assessed colonic sensitivity via a visceromotor response (VMR) to isobaric graded pressures of tonic colorectal distension (CRD) in freely moving animals.

Our findings confirmed that daily exposure to a psychological stressor induces colonic hypersensitivity in a rodent model. We then advanced these observations by providing novel experimental support to suggest that stress induces visceral pain, in part, through a mechanism involving microglia-mediated neuronal remodeling in the CeA via p38 MAPK activation and GR dysfunction.

Results


Daily WAS Increases Fecal Pellet Output and Induces Colonic Hypersensitivity

Animals subjected to WAS 1 hour per day for 7 consecutive days showed an increased number of fecal pellets during WAS (*Figure 1B*) ($n = 10$; $P < .0001$) and mean fecal pellet output (FPO) (*Figure 1C*) ($P < .0001$) as compared with SHAM. This significant increase of FPO suggests that animals did not habituate to the repetitive WAS procedure. Animals subjected to WAS also showed a greater VMR at distension pressures of 40 mm Hg ($n = 10$; $P = .0033$) and 60 mm Hg ($P < .0001$) as compared with SHAM controls (*Figure 1D*).

Morphologic Characterization of Microglial Plasticity in the CeA After Repeated WAS

To examine the plasticity of microglia in the CeA after exposure to chronic stress, microglia were labeled using a microglial-specific marker, Ionized calcium binding adaptor molecule 1 (Iba-1)²² (*Figure 2A and B*), and the microglial morphology was classified into 4 subtypes: ramified, primed, reactive, and amoeboid.²³ Ramified microglia were characterized as highly branched cell processes (*Figure 2C and D*, arrows) with small cell bodies, whereas activated microglia possessed thickened and retracted branches with enlarged cell bodies (*Figure 2C–F*).²⁴ Animals subjected to WAS had a

Abbreviations used in this paper: ANOVA, analysis of variance; CeA, central nucleus of the amygdala; CNS, central nervous system; CORT, corticosterone; CRD, colorectal distension; CRF, corticotropin-release factor; FPO, fecal pellet output; GR, glucocorticoid receptor; IBS, irritable bowel syndrome; IL, interleukin; mRNA, messenger RNA; PBS, phosphate-buffered saline; PCR, polymerase chain reaction; phospho-p38 MAPK, phosphorylated p38 mitogen-activated protein kinase; PSD95, postsynaptic density protein 95; TNF, tumor necrosis factor; WAS, water avoidance stress; VMR, visceromotor behavioral response.

 Most current article

© 2020 The Authors. Published by Elsevier Inc. on behalf of the AGA Institute. This is an open access article under the CC BY-NC-ND license (<http://creativecommons.org/licenses/by-nc-nd/4.0/>).

2352-345X

<https://doi.org/10.1016/j.jcmgh.2020.04.020>

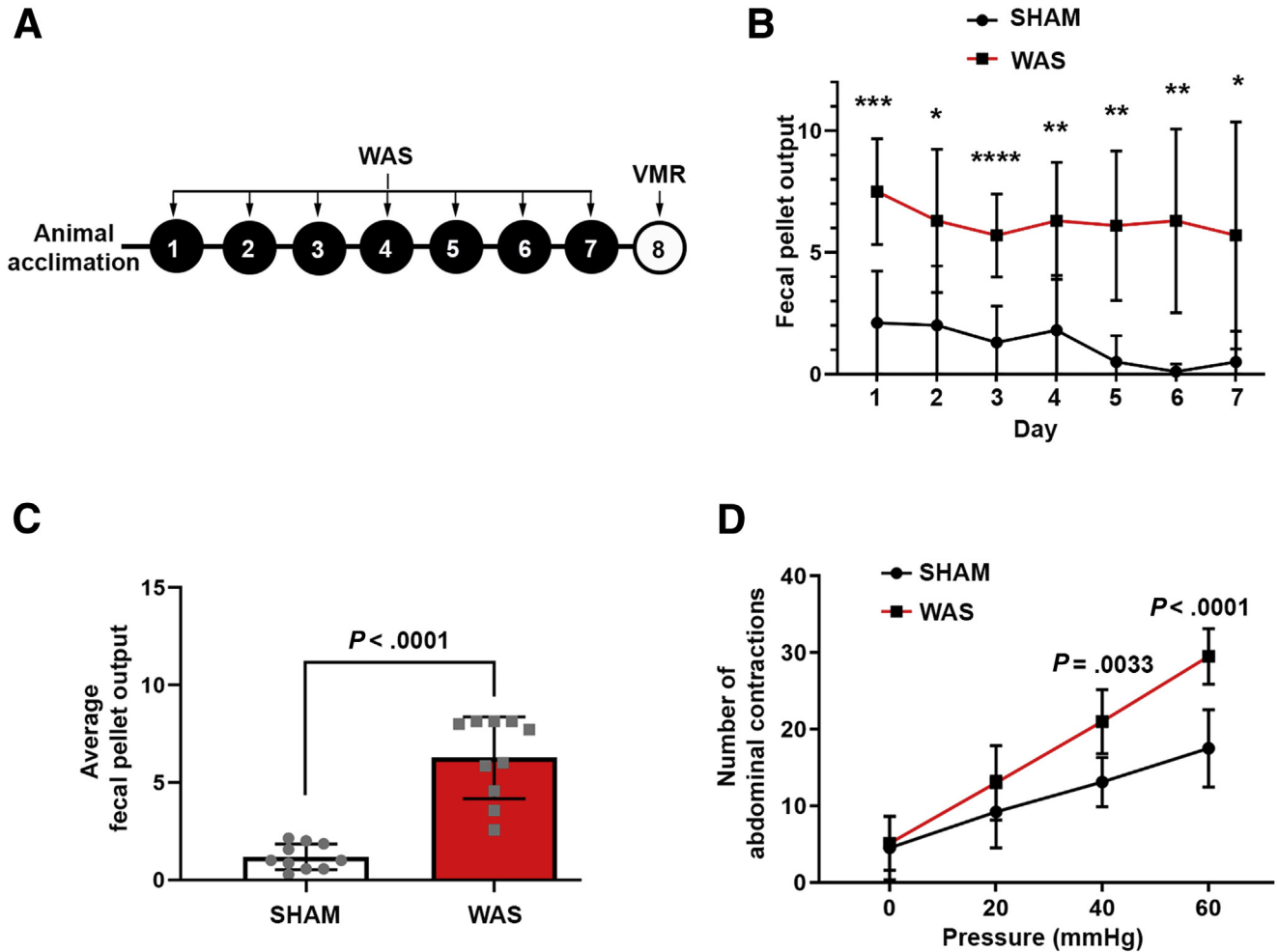
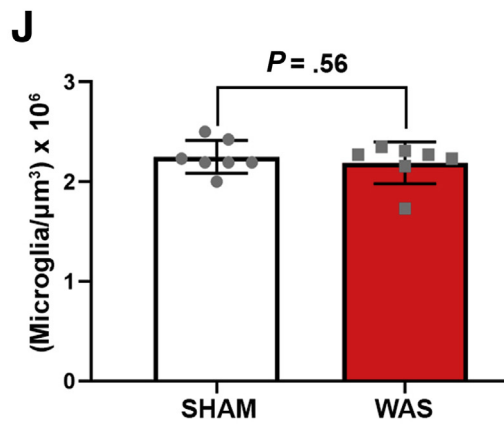
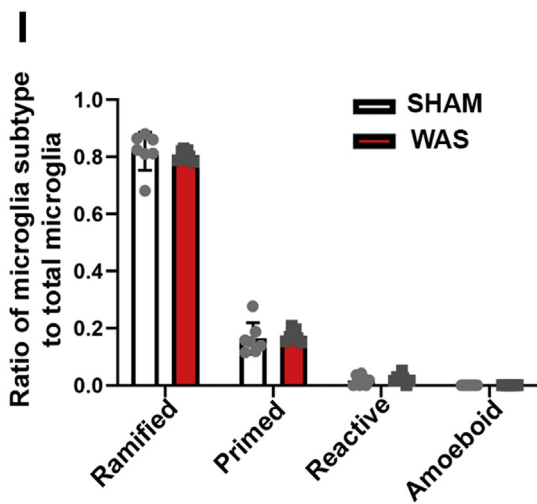
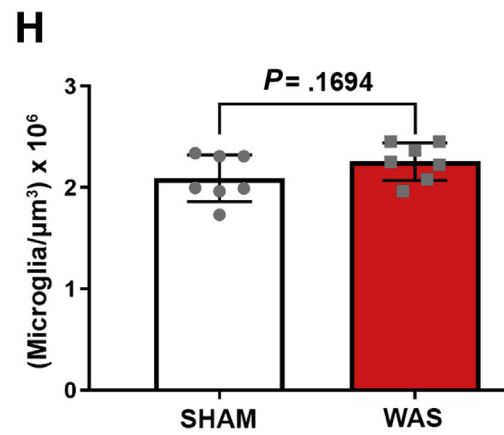
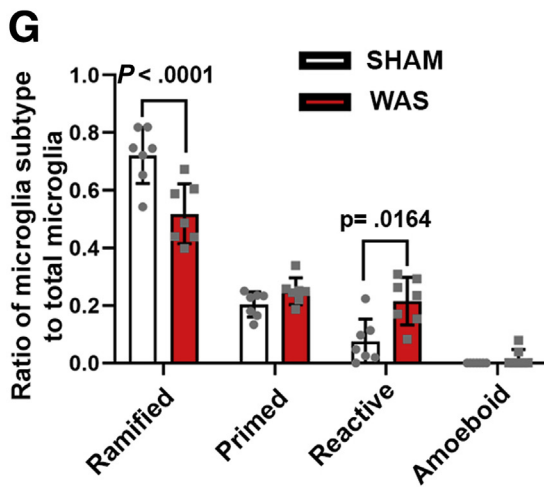
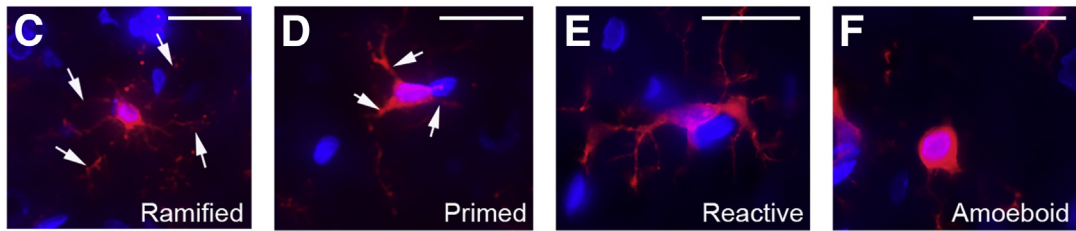
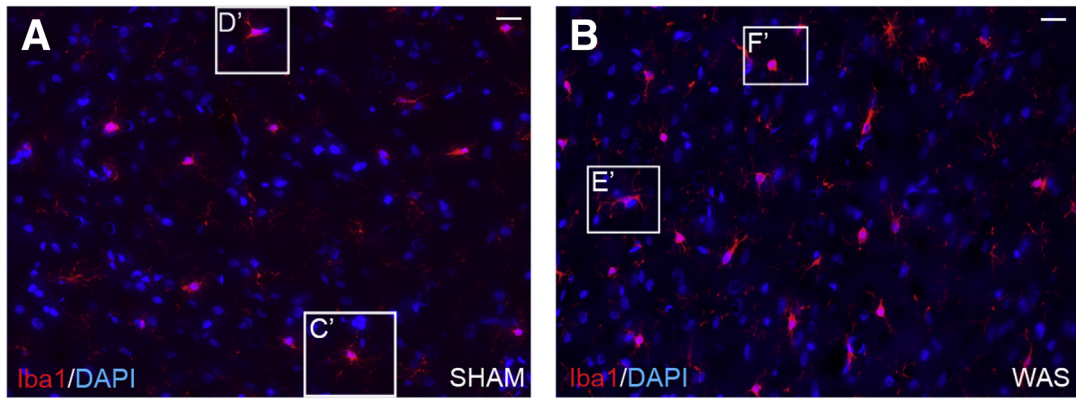


Figure 1. Repeated WAS induced visceral hypersensitivity in rats. (A) The in vivo experimental design. (B) Daily FPO ($n = 10$ per group, all $P < .05$). (C) Average FPO over 7 days. (D) Visceral sensitivity was assessed by quantification of abdominal contractions in response to tonic CRD ($n = 10$ per group). Data are presented as the means \pm SD. * $P < .05$, ** $P < .01$, *** $P < .001$, **** $P < .0001$.

smaller ratio of ramified microglia ($n = 7$; $P < .0001$) and a greater ratio of reactive microglia ($P = .0164$) as compared with control (Figure 2G). However, no change was observed in the total number of microglia between WAS and SHAM (Figure 2H) ($n = 7$; $P = .1694$). To examine whether chronic WAS induced microglial morphologic changes that are specific to the CeA, we investigated microglial morphology in the caudate putamen, which is not involved in the central regulatory circuit of stress-induced visceral pain.²⁵ Our data showed that there was no change in microglial morphology ($n = 7$; all $P > .05$) or density ($n = 7$; $P = .56$) in the caudate putamen after exposure to WAS compared with SHAM controls (Figure 2I and J). To investigate CeA microglial morphology after WAS exposure further, soma size (Figure 3A and B) and process occupied area (Figure 3D and E) also were measured. Compared with SHAM, exposure to WAS increased the mean soma size of microglia in the CeA (Figure 3C) ($n = 7$; $P = .0002$) and decreased their process outgrowth area (Figure 3F) ($n = 7$; $P < .0001$). All of these observations indicate that chronic WAS induced microglial deramification in the CeA.

WAS Increased Microglial Phospho-p38 MAPK Expression in CeA

To investigate whether microglial p-38 is activated in the CeA after WAS, we co-labeled phosphorylated-p38 (phospho-p38) with Iba-1. After exposure to chronic WAS, an increase in phospho-p38 expression in the CeA was observed compared with SHAM (compare Figure 4A and G). In the merged images, increased phospho-p38-positive microglia were observed (Figure 4A-C and G-I, arrows; and D-F and J-L). In the quantification analysis, the phospho-p38-positive area in the microglia was increased significantly in the CeA (Figure 4M) ($n = 7$; $P < .0001$), suggesting that repeated WAS activated microglial p-38 MAPK in the CeA. In addition to microglia, we also observed an increase in phospho-p38 expression in Iba-1-negative cells (Figure 4A, C, G, I, arrowheads). To identify the Iba-1-negative cells expressing phospho-p38, we co-labeled them with neuron marker Neuronal Nuclei and astrocyte marker glial fibrillary acidic protein. In the CeA, phospho-p38 was expressed in neurons



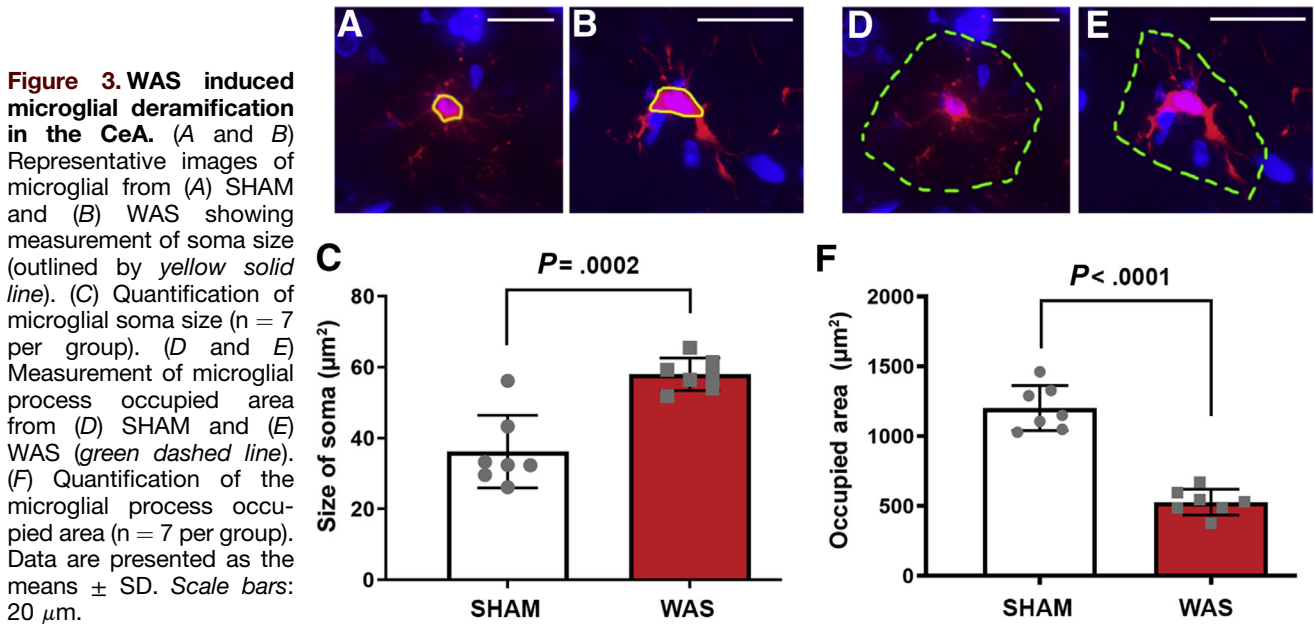


(Figure 4N–R) but not astrocytes (Figure 4T–X). Quantitative analysis showed that after exposure to chronic WAS, the expression of phospho-p38 was increased in neurons in the CeA (Figure 4S) ($n_{\text{SHAM}} = 6$, $n_{\text{WAS}} = 7$; $P = .0005$). This observation suggests that chronic stress activated p38 MAPK expression in both microglia and neurons.

WAS Compromised Microglial GR Translocation in the CeA

Ligand-bound GR undergoes translocation from the cytoplasm to the nucleus and functions as a transcription factor, whereas phospho-p38 inhibits GR nuclear translocation.^{26,27} Here, we examined whether chronic stress altered microglial GR expression in the CeA by examining the GR subcellular localization. Double immunofluorescence labeling of Iba-1 and GR was conducted and the expression ratio of GR in the cytoplasm (co-localizes with Iba-1) and in the nucleus (co-localizes with 4',6-diamidino-2-phenylindole) were measured. After exposure to 7-day WAS, the cytoplasmic GR ratio was increased significantly compared with SHAM, whereas nuclear GR was decreased (Figure 5A–F and quantified in G) ($n = 5$; $P = .0041$). These data indicate that exposure to chronic WAS compromised microglial GR nuclear translocation in the CeA.

WAS Increased Microglia-Mediated Synaptic Remodeling Without Changing Proinflammatory Cytokine Messenger RNA or Protein Levels in the CeA

Activated microglia have been reported to affect neuronal activity through modifying synapse density directly.²⁸ To examine whether chronic stress-induced microglial activation contributes to synaptic plasticity in the CeA, the post-synaptic protein marker postsynaptic density protein 95 (PSD95) was co-labeled with Iba-1 (Figure 6A–P). The number of PSD95-positive puncta in each microglia through all slices of the z-stack image was quantified after exposure to WAS or SHAM. In the SHAM animals, PSD95-positive post-synaptic spines were adjacent to, but not co-localized within, Iba-1-positive microglia (Figure 6A–E, arrowheads, generated maximum intensity projection image in 6F–H), whereas in animals exposed to chronic WAS increased postsynaptic spines were observed within the microglial process and cell body (Figure 6I–M, arrows, generated maximum intensity projection image in 6N–P; quantification in 6Q) ($n_{\text{SHAM}} = 6$, $n_{\text{WAS}} = 7$; $P < .0001$). This result suggests that after chronic WAS exposure, microglia-mediated engulfment of post-synaptic spine was increased in the CeA.

In addition to synaptic remodeling, activated microglia release cytokines to regulate neuronal activity.²⁹ To investigate whether WAS-induced microglial activation has any

Figure 2. (See previous page). WAS altered microglial morphology in the CeA. (A and B) Iba-1/4',6-diamidino-2-phenylindole (DAPI) (red/blue) immunofluorescence staining in the CeA of (A) SHAM and (B) WAS animals. (C–F) Enlarged images of representative (C) ramified, (D) primed, (E) reactive, and (F) amoeboid subtypes in panels A and B. Arrows in C and D point to microglial processes. C–F are higher magnification of C'–F' in panels A and B. (G) Ratio of microglial subtypes in the CeA after exposure to SHAM or WAS. (H) Quantification of microglial cell density in the CeA (n = 7 per group). (I) Ratio of microglial subtypes in the caudate putamen after exposure to SHAM or WAS. (J) Quantification of microglial cell density in the caudate putamen (n = 7 per group). Data are presented as the means \pm SD. Scale bars: 20 μ m.

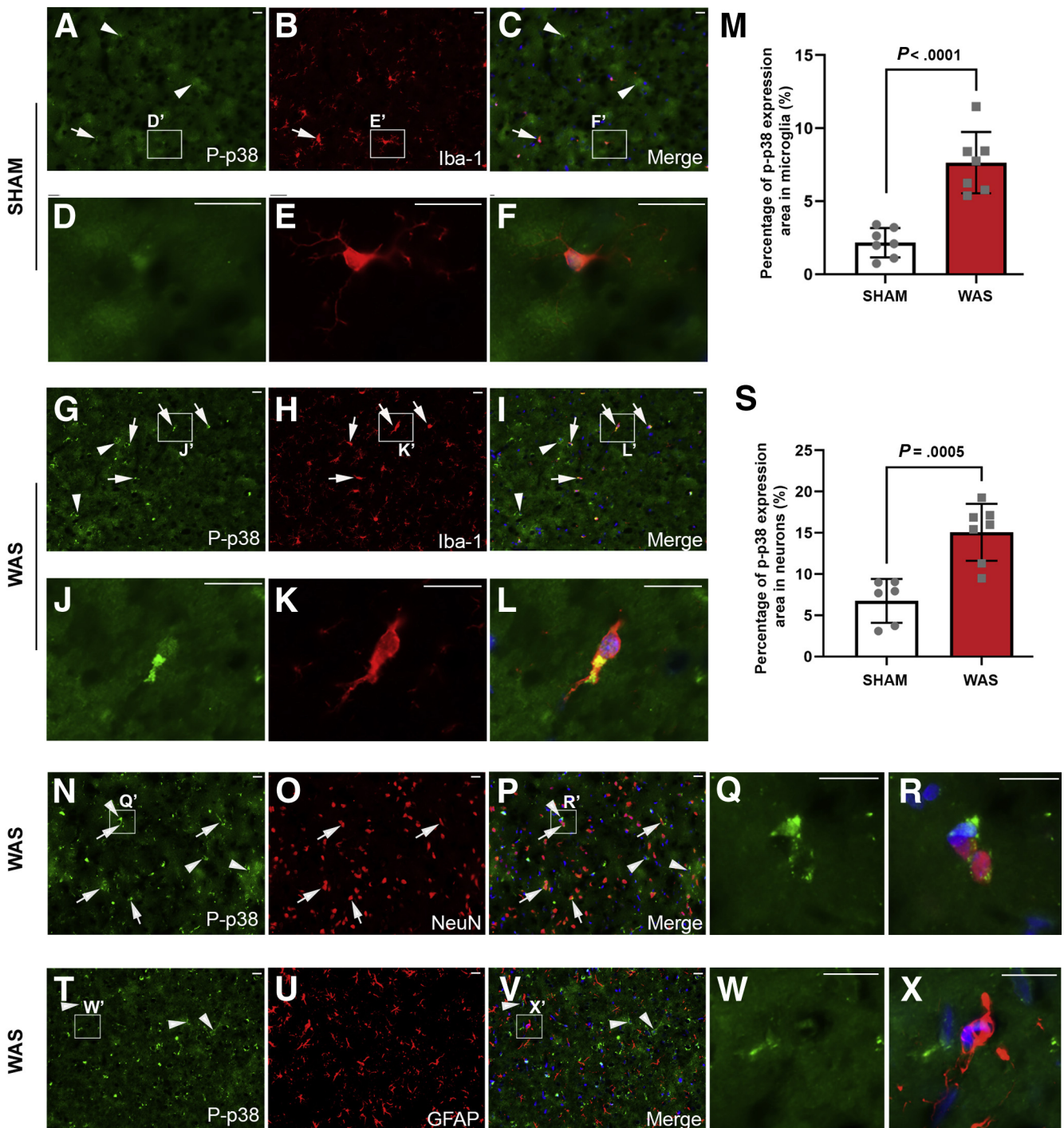


Figure 4. WAS increased microglial phospho-p38 MAPK expression in the CeA. (A–L) Co-labeling of phospho-p38 (green) with Iba-1 (red) in the CeA of (A–F) SHAM and (G–L) WAS animals showing phospho-p38 expression in microglia (arrows) and Iba-1-negative cells (arrowheads). (D–F) Higher magnification of boxed areas in panels A–C. (J–L) Higher magnification of boxed areas in panels G–I. (M) Quantification of phospho-p38 expression (% volume) in Iba-1-positive cells ($n = 7$ per group). (N–R) Co-labeling of phospho-p38 (green) with Neuronal Nuclei (NeuN) (red) showing phospho-p38 expression in neurons (arrows) and non-neuronal cells (arrowheads). (S) Quantification of phospho-p38 expression (% volume) in neurons. $n_{\text{SHAM}} = 6$, $n_{\text{WAS}} = 7$. (T–X) Co-labeling of phospho-p38 (green) with glial fibrillary acidic protein (GFAP) (red) showing phospho-p38 expression in GFAP-negative cells (arrowheads). (Q, R, W, and X) Higher magnification of boxed regions in panels N, P, T, and V, respectively. Data are presented as the means \pm SD. Scale bars: 20 μm .

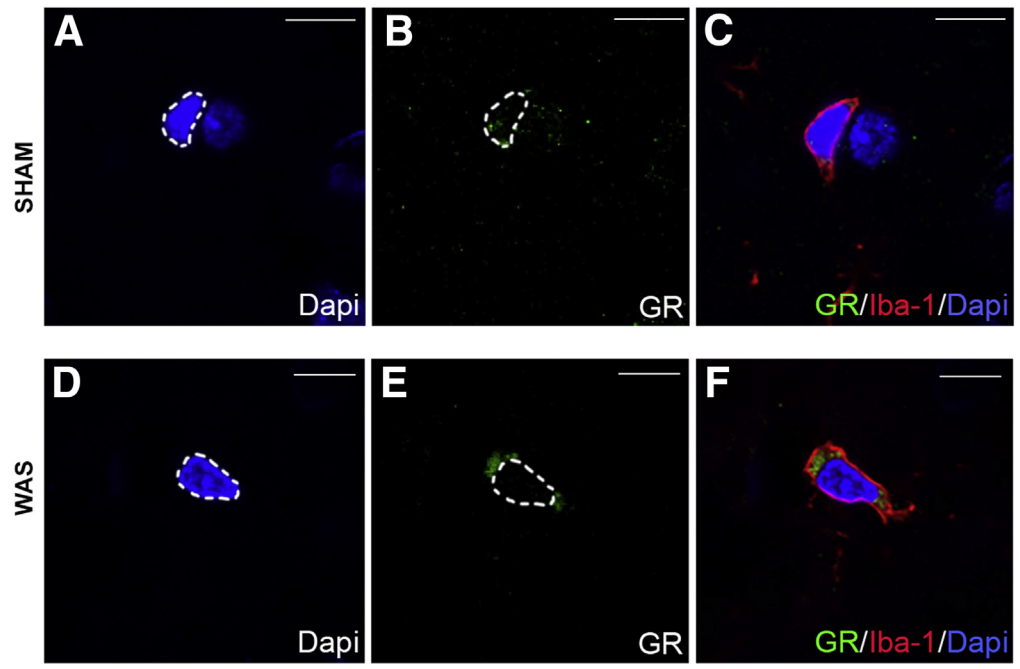
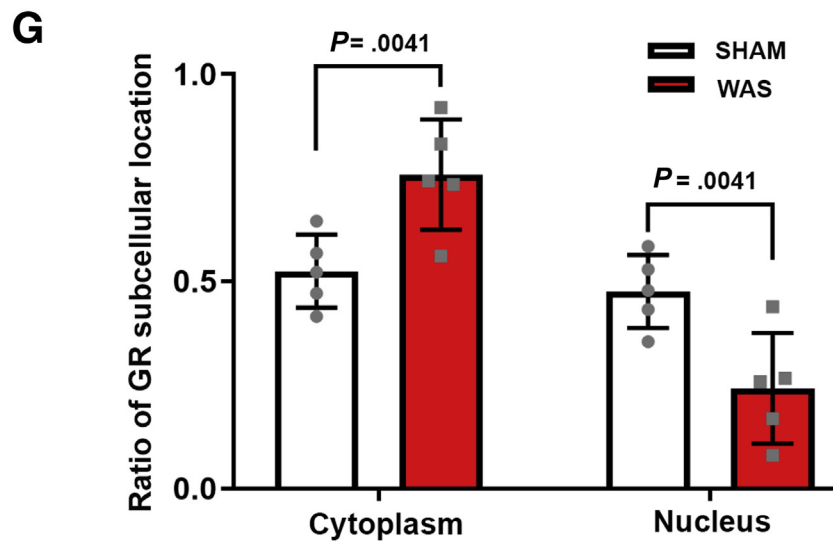


Figure 5. WAS inhibited microglial GR nuclear translocation in the CeA. (A–F) Selected slices from z-stack images show co-labeling of GR (green) with Iba-1 (red) in the CeA of (A–C) SHAM and (D–F) WAS animals. The white dashed line indicates the outline of nuclei (4',6-diamidino-2-phenylindole [DAPI] staining). (G) Ratio of microglial GR expression in the cytoplasm and nucleus ($n = 5$ per group). Data are presented as the means \pm SD. Scale bars: 10 μ m.



effect on the messenger RNA (mRNA) production of the proinflammatory cytokines in the CeA, quantitative polymerase chain reaction (PCR) was conducted to measure the expression of interleukin (IL) 1β , tumor necrosis factor (TNF) α , and IL6. After exposure to repeated WAS, mRNA level of IL 1β ($n = 10$; $P = .71$), TNF α ($n = 10$; $P = .51$), or IL6 ($n_{\text{SHAM}} = 4$, $n_{\text{WAS}} = 6$; $P = .81$) was not changed in the CeA (Figure 6R–T). In light of this unchanged cytokine profile we quantified cytokine protein production in the CeA via a Luminex assay for 23 cytokines (Bio-Rad, Hercules, CA). After WAS exposure, no change was observed in all 23 measured cytokine proteins, including IL 1β , TNF α , and IL6 (Figure 6U–W, Table 1) ($n = 6$; $P_{\text{IL}1\beta} = 0.61$, $P_{\text{TNF}\alpha} = .85$, $P_{\text{IL}6} = .37$), which confirmed our transcription data from quantitative PCR analysis. This result suggests that cytokine

production in the CeA was not affected after exposure to chronic WAS.

Minocycline Reverses Stress-Induced Visceral Hypersensitivity and Inhibited Stress-Induced Microglial Activation and Microglia-Mediated Synaptic Remodeling

To examine whether the activation of microglia in CeA is responsible for stress-induced visceral hypersensitivity, we used a pharmacologic approach in which microglia activity was inhibited by direct stereotaxic infusion of minocycline into the CeA preceding daily WAS exposure (Figure 7A and B). Our data suggest that daily infusions of minocycline into the CeA before WAS exposure was sufficient to inhibit

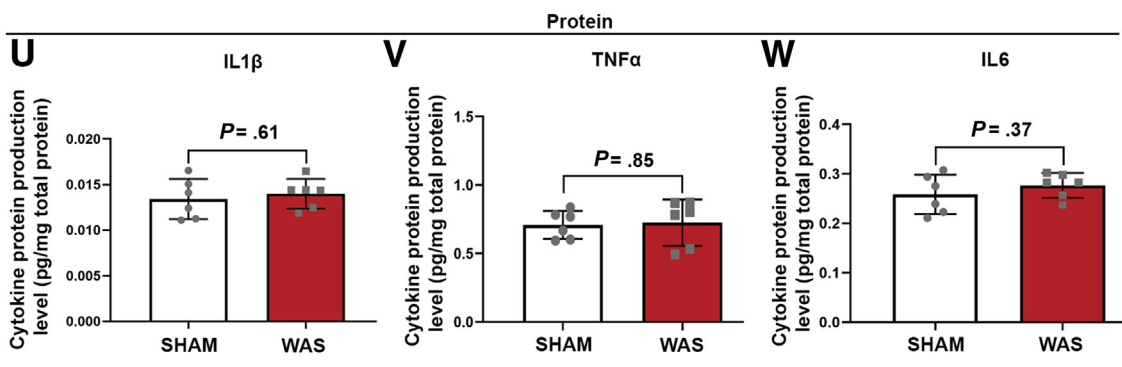
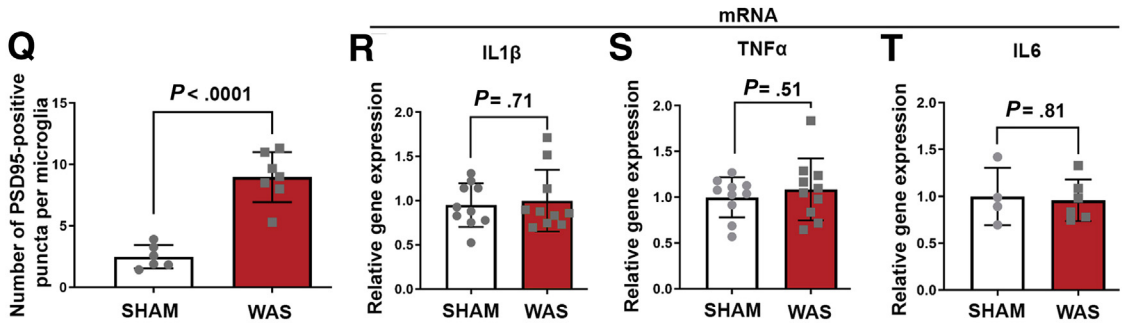
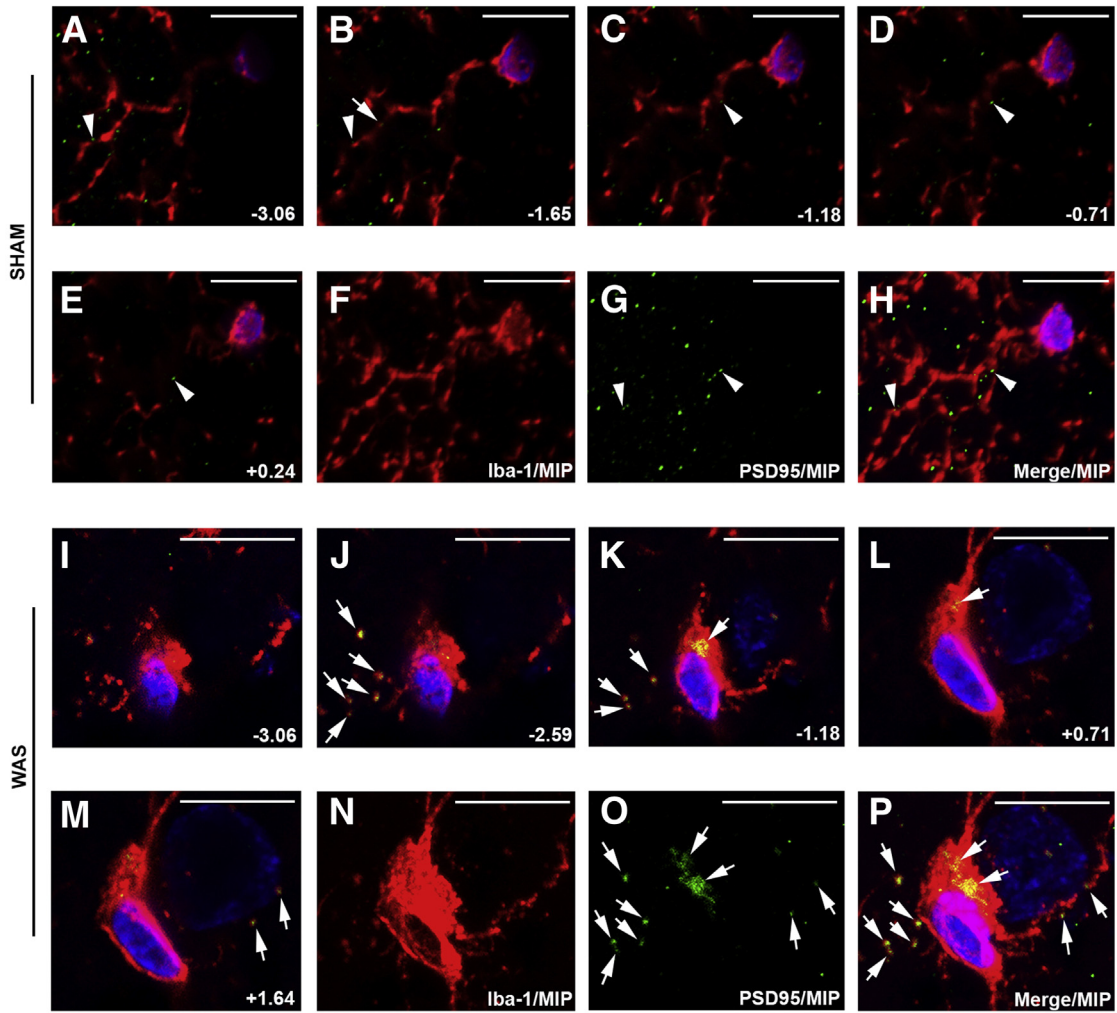


Table 1. Cytokine Protein Levels in the CeA After Exposure to WAS

	SHAM	WAS	P value		SHAM	WAS	P value
IL1 α	0.011 \pm 0.004	0.011 \pm 0.001	.91	MCSF	0.012 \pm 0.002	0.012 \pm 0.001	.94
IL2	18.328 \pm 6.459	15.072 \pm 2.290	.27	GCSF	0.016 \pm 0.002	0.015 \pm 0.003	.71
IL4	0.017 \pm 0.002	0.016 \pm 0.001	.44	VEGF	0.046 \pm 0.018	0.049 \pm 0.011	.72
IL5	0.024 \pm 0.027	0.023 \pm 0.017	.93	GMCSF	0.132 \pm 0.030	0.114 \pm 0.024	.29
IL7	0.230 \pm 0.120	0.189 \pm 0.066	.49	GRO KC	0.015 \pm 0.005	0.015 \pm 0.005	.90
IL10	0.022 \pm 0.005	0.021 \pm 0.004	.74	RANTES	0.044 \pm 0.011	0.046 \pm 0.008	.70
IL12p70	0.251 \pm 0.062	0.262 \pm 0.038	.71	Interferon- γ	0.115 \pm 0.016	0.110 \pm 0.017	.61
IL13	0.095 \pm 0.026	0.097 \pm 0.017	.86	MCP-1	0.161 \pm 0.024	0.165 \pm 0.034	.82
IL17 α	0.112 \pm 0.021	0.116 \pm 0.011	.63	MIP-1a	0.005 \pm 0.002	0.005 \pm 0.001	.97
IL18	1.900 \pm 0.176	1.889 \pm 0.195	.92	MIP-3a	0.004 \pm 0.001	0.004 \pm 0.0002	.79

NOTE. Values of cytokine levels are in pg/mg total protein. Means \pm SD are shown. n = 6/group. Statistics were assessed by unpaired *t* test.

GCSF, granulocyte-colony stimulating factor; GMCSF, granulocyte-macrophage colony-stimulating factor; GRO KC, growth related oncogene; MCP-1, monocyte chemoattractant protein-1; MCSF, macrophage colony-stimulating factor; MIP, macrophage inflammatory proteins; RANTES, regulated on activation, normal T cell expressed and secreted.

microglial activation and reverse the stress-induced visceral hypersensitivity (Figure 7C) ($n_{\text{WAS+vehicle}} = 6$, $n_{\text{WAS+minocycline}} = 10$; $P_{20\text{mm Hg}} = .0005$, $P_{40\text{mm Hg}} = .002$, $P_{60\text{mm Hg}} < .0001$), indicating the role of microglia in limbic brain-mediated visceral hypersensitivity.

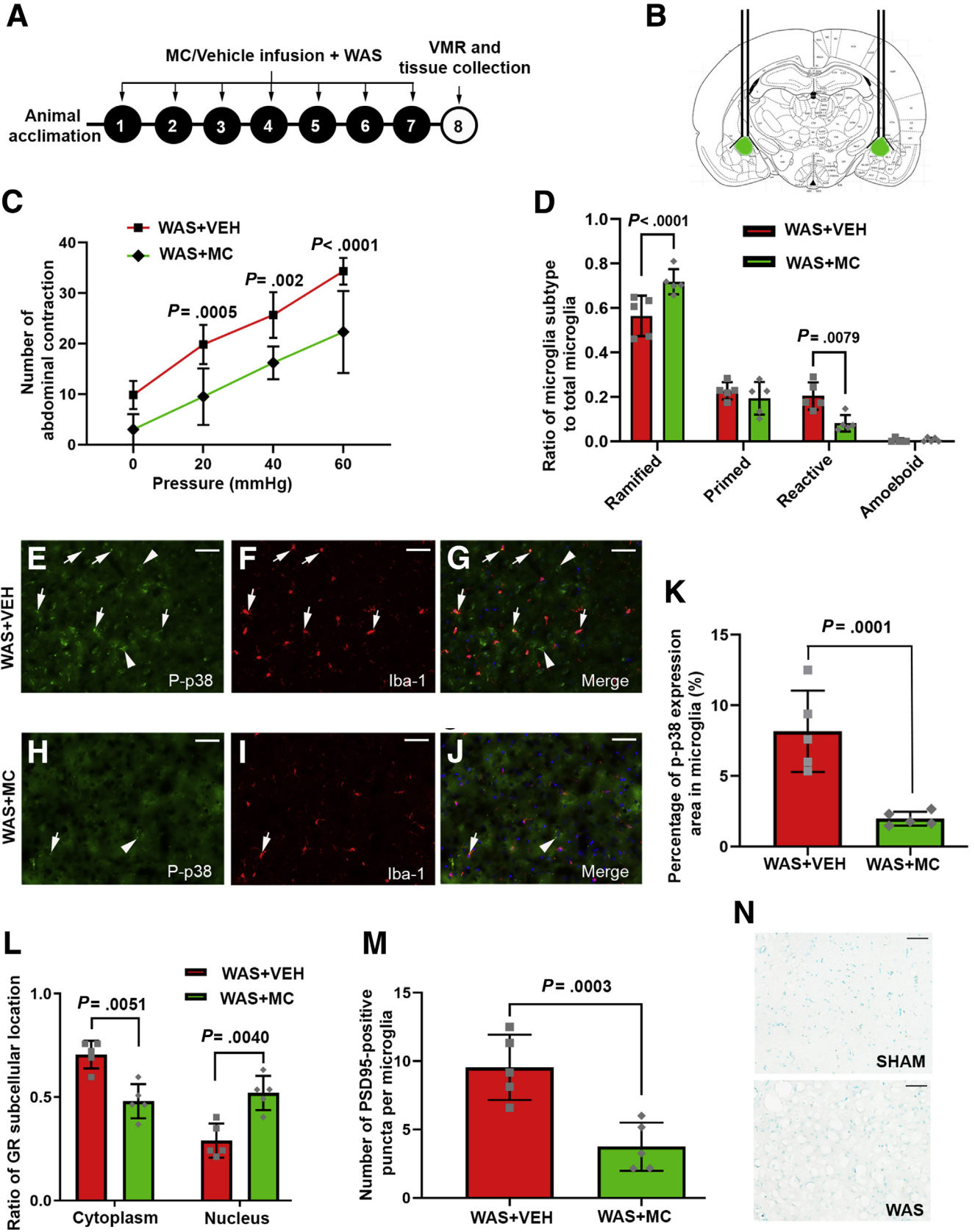
To investigate whether microglial activity was altered by minocycline after exposure to chronic stress, microglial morphology as well as phospho-p38 expression was examined. After 7 days of infusion, minocycline decreased the ratio of reactive microglial subtypes ($n = 5$; $P = .0079$) and increased the ratio of ramified microglia ($P < .0001$) in the WAS group compared with the vehicle-infused animals (Figure 7D). Furthermore, infusion of minocycline into CeA was sufficient to decrease microglial phospho-p38 expression in response to WAS (Figure 7E-K) ($n = 5$; $P = .0001$). Phospho-p38 MAPK inhibits GR nuclear translocation via blocking its ligand binding site.²¹ To investigate whether infusion of minocycline also reversed stress-induced GR cytoplasmic accumulation, GR expression in microglial cytoplasm and in the nucleus was examined. In WAS-exposed animals, infusion of minocycline decreased the ratio of cytoplasmic GR expression ($n = 5$; $P = .0051$), and increased nuclear GR expression ($P = .004$) in the CeA compared with vehicle-infused animals (Figure 7L). Furthermore, to investigate microglia-mediated synaptic remodeling after administration of minocycline, PSD95-positive puncta in each microglia were quantified. Infusion of minocycline decreased the number of postsynaptic spines in each microglia ($n = 5$; $P = .0003$) in the CeA of WAS animals, suggesting that microglia-mediated synaptic engulfment was attenuated by minocycline (Figure 7M). To eliminate the

possibility that minocycline decreased visceral sensitivity through protecting neurons from cell death,³⁰⁻³² we applied apoptosis analysis in the CeA from animals in the WAS and SHAM groups. No cell death was apparent in the CeA from WAS- and SHAM-treated animals (Figure 7N) ($n = 5$), suggesting that minocycline administration in the CeA eliminated stress-induced visceral hypersensitivity by decreasing microglial activity, rather than preventing neuronal apoptosis.

Fractalkine Increased Visceral Sensitivity and Induced Microglial Morphologic Alteration and Phospho-p38 Up-Regulation in SHAM Rats

To further associate microglial activation in the CeA to the development of visceral hypersensitivity, a microglial activator, fractalkine was infused stereotaxically into the CeA. After 7 days of infusion in SHAM-stressed rats (Figure 8A), fractalkine induced visceral hypersensitivity (Figure 8B) ($n = 6$; $P_{20\text{mm Hg}} = .0145$, $P_{40\text{mm Hg}} = .0003$, $P_{60\text{mm Hg}} < .0001$), in comparison with vehicle-infused SHAM animals. To examine whether fractalkine infusion activated microglia, we examined microglial morphology as well as microglial phospho-p38 expression in the CeA. Fractalkine decreased ramified ($n = 6$; $P < .0001$) and increased reactive ($P < .0001$) microglial subtypes in the CeA (Figure 8C). Fractalkine also increased phospho-p38 expression in the microglia compared with vehicle-infused SHAM rats (Figure 8D and E-J, arrows) ($n = 6$; $P < .0001$). These results indicate that activating microglia in the CeA is sufficient to induce visceral hypersensitivity in nonstressed animals.

Figure 6. (See previous page). WAS exposure increased synaptic engulfment by microglia in the CeA. (A-P) Co-labeling of PSD95 (green) with Iba-1 (red) in the CeA of (A-H) SHAM and (I-P) WAS animals. (A-E and I-M) Selected slices from z-stack images indicate PSD95-positive puncta overlapping (arrows) or not overlapping with (arrowheads) Iba-1. The numerals in the lower right corner in each panel indicate the distance (μm) below (-) or above (+) the center focal plane of the z-stack image. (F-H and N-P) Generated maximum intensity projection (MIP) images. (Q) Quantification of PSD95-positive puncta in Iba-1-positive cells. $n_{\text{SHAM}} = 6$, $n_{\text{WAS}} = 7$. (R-T) Quantitative PCR analysis showing the relative mRNA expression level of IL1 β ($n = 10$ per group), TNF α ($n = 10$ per group), and IL6 ($n_{\text{SHAM}} = 4$, $n_{\text{WAS}} = 6$) in the CeA. (U-W) IL1 β , TNF α , and IL6 concentration in the CeA ($n = 6$ per group). Data are presented as the means \pm SD. Scale bars: 10 μm .



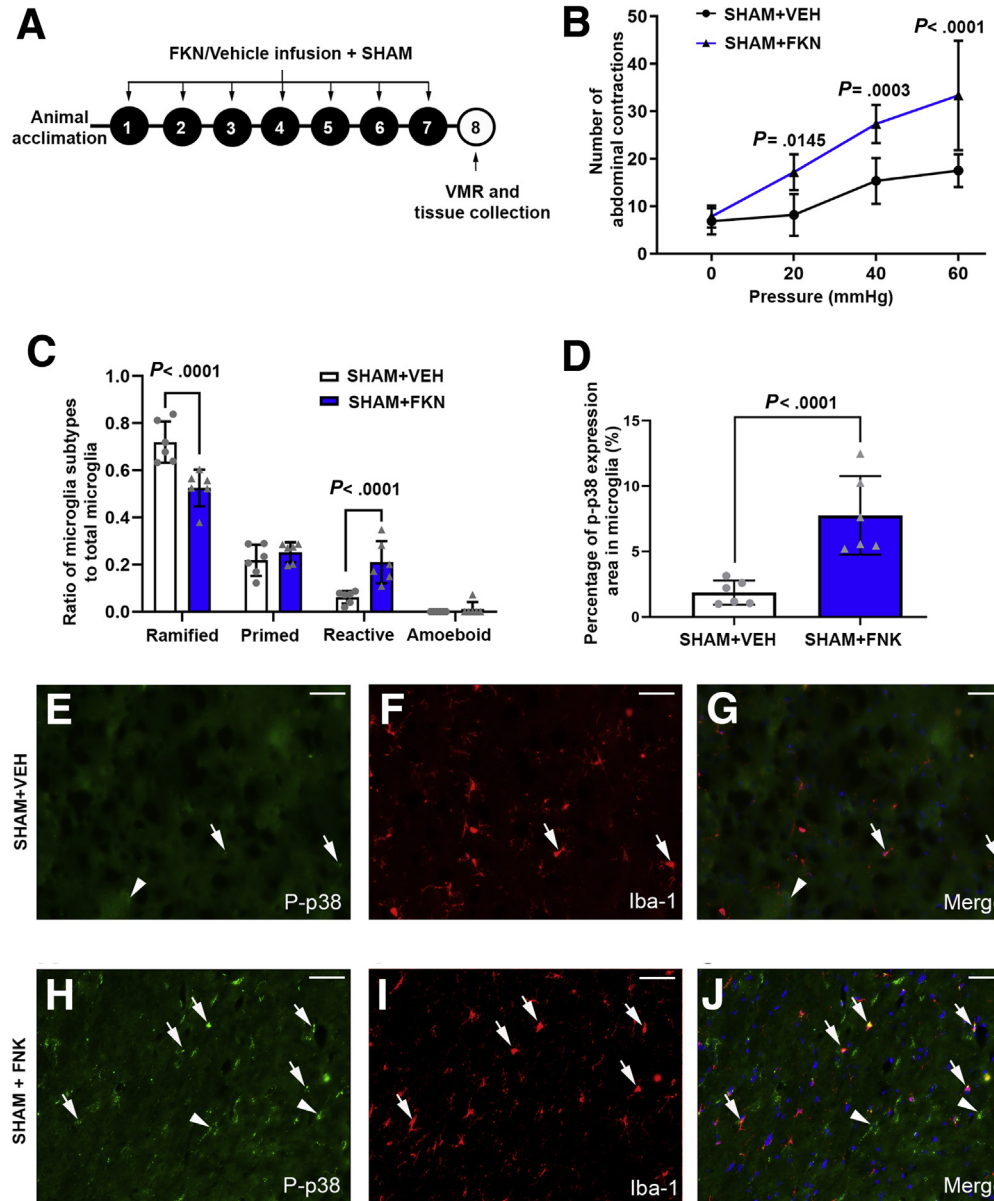


Figure 8. Infusion of fractalkine into CeA-induced microglial deramification and visceral hypersensitivity in stress-naïve animals ($n = 6$ per group). (A) The experimental design. (B) VMR to CRD of vehicle- or fractalkine- (FNK) infused animals after exposure to SHAM. (C) Ratio of microglial subtypes in the CeA. (D) Quantification of phospho-p38 expression (volume %) in microglia in the CeA. (E–J) Representative immunofluorescence images of phospho-p38 (green) co-labeling with Iba-1 (red) showing phospho-p38 expression in Iba-1-positive (arrows) and Iba-1-negative (arrowheads) cells after infusion of (E–G) vehicle or (H–J) fractalkine. Data are presented as the means \pm SD. Scale bars: 50 μ m. VEH, vehicle.

Discussion

Our previous research showed that the limbic brain, specifically the CeA, is implicated strongly in the development of stress-induced visceral hypersensitivity.^{8,33} However, the cellular mechanisms within the CeA driving visceral

hypersensitivity remain to be elucidated. In the current study, our goal was to test the hypothesis that microglia in the CeA contribute to chronic stress-induced visceral nociceptive processing. Microglia in the limbic brain has been associated previously with stress-induced anxiety and depressive-like behaviors, while spinal microglia contribute to chronic

Figure 7. (See previous page). Infusion of minocycline into CeA reversed stress-induced microglial deramification and visceral hypersensitivity. (A) Experimental design. (B) Illustrated image showing the cannula position above the CeA and delivery of vehicle or minocycline into CeA. (C) VMR to CRD in vehicle- (VEH) and minocycline- (MC) infused animals after WAS. $n_{WAS+VEH} = 6$ per group, $n_{WAS+MC} = 10$ per group. (D) Ratio of microglial subtypes in the CeA of vehicle- or minocycline-infused animals after exposure to WAS. (E–J) Co-labeling of phospho-p38 (green) and Iba-1 (red) in the CeA showing phospho-p38 expression in Iba-1-positive (arrows) and Iba-1-negative (arrowheads) cells after infusion of (E–G) vehicle- and (H–J) minocycline. (K) Quantification of phospho-p38 expression (% volume) in microglia ($n = 5$ per group). (L) Ratio of GR expression in the cytoplasm and nucleus after vehicle or minocycline infusion ($n = 5$ per group). (M) Quantification of PSD95-positive puncta in Iba-1-positive cells in the CeA ($n = 5$ per group) (N) Representative images of apoptosis assay in the CeA of SHAM and WAS animals ($n = 5$ /group). Data are presented as the means \pm SD. Scale bars: 50 μ m.

stress-induced visceral pain.^{18,34–37} However, the current study shows that microglia in the amygdala, specifically the CeA, regulate visceral nociception after exposure to chronic psychological stress. In our initial studies we found that after repetitive daily exposure to water avoidance, microglia in the CeA undergo a morphologic change to become deramified. In addition to morphologic alteration, we also found increased microglial phospho-p38 MAPK expression and a decreased ratio of nuclear GR, indicating the potential molecular mechanisms involved in the microglia structural and functional plasticity that are associated with stress response. Moreover, the number of postsynaptic marker PSD95-positive puncta in the microglia was increased in the CeA from stressed animals, suggesting a microglia-mediated synaptic remodeling. Although these findings were sufficient to highlight an important role for microglia in the CeA in response to chronic stress, our next experiments aimed to assess whether the deramified microglia in the CeA contribute to stress-induced nociceptive behavior. We showed that microinfusion of minocycline (a microglial inhibitor) directly into the CeA reversed the microglial morphologic change, prevented the microglia-mediated synaptic engulfment, and reversed the visceral hypersensitivity induced by chronic stress. Conversely, infusion of fractalkine (a microglial activator) induced microglial remodeling and colonic hypersensitivity in nonstressed rats (SHAM). Taken together, our results provide compelling evidence that chronic stress induces microglial structural and functional remodeling in the amygdala to mediate visceral nociceptive behaviors. These findings show an important role of supraspinal microglia in stress-induced brain and gut dysfunction, providing a novel potential target in treating IBS patients with visceral pain that is worsened during episodes of stress.

In the current study, we specifically focused on microglial plasticity in the CeA. We selected this brain region based on prior evidence from our laboratory as well as from others suggesting that the CeA is a key brain region that regulates both stress and visceral nociceptive responses.^{7,38–40} In rats, we found that exposure of the CeA to increased levels of CORT was sufficient to induce visceral hypersensitivity as well as decrease GR and increase corticotropin-release factor (CRF) expression.^{25,41,42} In the WAS model, similar changes in GR and CRF expression were observed, while CRF knockdown in the CeA inhibited stress-induced visceral hypersensitivity, suggesting the CeA serves a critical function in regulating visceral nociception.⁸ In the current study we showed that changes in microglial morphology and neuronal remodeling in the CeA was sufficient to induce visceral hypersensitivity, whereas infusion of a microglia inhibitor into the CeA reversed WAS-induced visceral hypersensitivity, pointing to the pivotal involvement of amygdala microglia in stress-induced visceral pain.

In an attempt to model a chronic psychological stressor, in the current study we exposed animals to repeated water avoidance, which has been associated with the development of colonic hypersensitivity to mechanical distension.^{6,8,12,13} Our results showed that after the exposure to WAS, microglia in the CeA transition from a ramified morphology with a small cell body and extended processes toward the more

reactive morphology with enlarged microglial soma size and decreased microglial process occupied area. In addition, we analyzed the total number of microglia in the CeA. Interestingly, we found no change in the total number of microglia between WAS-exposed animals and SHAM controls, suggesting that chronic WAS induced microglial deramification in CeA without increasing the cell number. In support, a previous study showed that chronic restraint stress alters the microglial density and morphology in multiple stress-responsive brain regions, whereas the amygdala showed no differences in microglia counts between control and stressed animals.⁴³

A number of previous studies have shown that p38 MAPK regulate microglial activity in the CNS in response to neuropathic pain and traumatic brain injury.^{44–46} However, to our knowledge, the role of p38 MAPK in the CeA in response to chronic psychological stress remains unexplored. Thus, in our next series of experiments we aimed to investigate whether activation of microglial p38 in the CeA occurs in response to chronic psychological stress. Our findings showed that chronic stress increased phospho-p38 MAPK expression in Iba-1-positive cells, which is consistent with previous reports in the spinal cord after injury or chronic stress.^{18,47} Our double immunofluorescence labeling showed that phospho-p38 also is expressed in neurons but not in astrocytes. Although we are not able to identify which cell type initially activated p38 MAPK in our model, one possibility is that after chronic stress, neuronal phospho-p38 expression is triggered by activated microglia. In the brain, activated microglia has been shown to modify synaptic elements by activating neuronal p38 MAPK.⁴⁸ However, with the current experimental design, we were not able to exclude the possibility that neuronal p38 MAPK was activated independently of microglial p38, and that this contributed to stress-induced visceral hypersensitivity.

We found that stereotaxic infusion of minocycline, a microglial inhibitor, into the CeA reversed stress-induced microglial phospho-p38 MAPK expression. This observation, together with our finding that minocycline attenuated stress-induced visceral hypersensitivity, supports our claim that suppressing the increase of phospho-p38 could be one of the mechanisms by which minocycline inhibits visceral hypersensitivity after exposure to chronic WAS. In support, microinfusion of fractalkine, a microglial activator, increased microglial phospho-p38 in the CeA and induced visceral pain in stress-naïve rats.

Minocycline is used commonly to inhibit microglial activation. However, minocycline also has been reported to directly affect neurons.^{32,49,50} Multiple lines of evidence have shown the role of minocycline in protecting neurons from apoptosis via inhibiting p38 MAPK activity.^{30–32,51,52} Our observation of increased neuronal p38 MAPK activity in the CeA raises the possibility that minocycline could have inhibited visceral hypersensitivity through an attenuation of neuronal apoptosis via a direct inhibition of p38 MAPK activity. Therefore, we applied apoptosis analysis in WAS and SHAM animals. According to our apoptosis analysis, WAS did not cause significant cell death in the CeA. Thus, it is unlikely that minocycline attenuated WAS-induced visceral hypersensitivity by protecting neurons from apoptosis.

During episodes of stress the body responds by releasing CORT, which serves as the ligand for GR and triggers GR translocation from the cytoplasm to the nucleus to regulate gene expression.⁵³ Previous studies have associated dysfunction of GR within the microglia with microglial morphologic change and microglia-mediated neuronal remodeling.^{20,54–56} Here, we report that repeated exposure to a WAS compromises microglial GR translocation to the nuclei in the CeA. Our laboratory already has shown that global knockdown of GR in the CeA induced visceral hypersensitivity in stress-naïve rats,^{39,41,57} however, the cellular mechanism of GR-mediated visceral pain was not investigated previously. Data from the current study suggest that a decreased ratio of microglial nuclear GR in the CeA may represent one of the mechanisms underlying stress-induced visceral hypersensitivity. Interestingly, phospho-p38 MAPK negatively regulates GR nuclear translocation by directly blocking the GR ligand-binding domain.^{21,27,58} Thus, we hypothesize that the observed p38 MAPK activation in the microglia contributes to the GR cytoplasmic accumulation after exposure to chronic stress. This hypothesis is supported by our observation of reversed GR cytoplasmic accumulation in animals exposed to WAS after infusion of minocycline, which inhibited p38 MAPK activation in the CeA.

Activated microglia are able to regulate neuronal activity through the modification of synaptic plasticity.^{28,59} We examined microglial engulfed postsynaptic spines in the CeA after WAS, and found increased PSD95-positive puncta in microglia, suggesting that deramified microglia increased their ability to contact and modify postsynaptic structures. Microglia contact and survey dendrite synapses in the healthy brain to maintain the proper function of synapses in neuron–neuron communication, whereas in the diseased brain, activated microglia have been associated with the loss of synapses.^{20,28,60–63} In our model, increased microglial engulfment of synaptic spines in the CeA combined with the observation of increased visceral sensitivity suggested an association between microglia-mediated neuronal remodeling in the CeA with the development of visceral hypersensitivity after exposure to chronic stress. In support, minocycline infusion into the CeA decreased microglia-mediated synaptic remodeling and decreased the visceromotor behavioral response to luminal distension, which further suggests a relationship between the functional plasticity of amygdala microglia with stress-induced visceral pain.

In addition to direct synaptic remodeling, activated microglia also regulate neuronal function by releasing inflammatory cytokines. Previous studies have shown increased proinflammatory cytokines in the hippocampus, prefrontal cortex, and hypothalamus after exposure to various forms of stress including footshock, restraint, or chronic stress induced by randomized exposure to water/food deprivation, temperature change, or swimming in cold water.^{35,36,64} We therefore examined the levels of 3 major proinflammatory cytokines in the CeA released by microglia, and our finding showed no change in TNF α , IL1 β , or IL6 mRNA, or protein levels in the CeA after exposure to chronic WAS. A potential explanation for why exposure to WAS induces microglial morphologic changes in the CeA without

increasing the release of proinflammatory cytokines may be that WAS is considered to be a more psychological stress model whereas footshock, restraint, and chronic mild stress models all include physical components. However, we cannot exclude the possibility of changes in the expression of other inflammatory cytokines, or that a change in inflammatory cytokines occurred at a time point different than at the time we conducted our analysis.

In conclusion, our new data highlight the mechanism by which chronic psychological stress causes microglial deramification within the amygdala. Hippocampal and hypothalamic microglia have been associated with neonatal colorectal distension-induced visceral hypersensitivity in adults,^{65,66} and we report that chronic psychological stress increases microglia-mediated synaptic remodeling to induce visceral pain via activation of p38 MAPK and inhibition of GR signaling without altering proinflammatory cytokine levels in the CeA. In summary, our study provides new insights into the supraspinal central pain circuitry modulated by exposure to chronic stress. A caveat in the interpretation of the current study is that all experiments were performed in male animals and thus directly extrapolating our findings to females requires further study. However, our findings are consistent with the view that stress has profound effects in the brain–gut axis, and that microglial plasticity and microglia-mediated synaptic remodeling participate in the pathogenesis of chronic stress-induced visceral pain.

Methods

Animals

Male Fischer 344 rats (weighing 250–350 g; Charles Rivers Laboratory, Wilmington, MA) were used in all experiments. This strain was chosen specifically for their inability to habituate to repeated chronic stress.⁸ Rats were double-housed unless they underwent stereotaxic surgery, after which animals were single-housed. All experiments were approved by the University of Oklahoma Health Sciences Center Institutional Animal Care and Use Committees under protocol 16-122-SS.

WAS

Rats were placed on a square platform (7 × 7 × 9 cm) mounted in the center of a white transparent plastic container (40 × 50 × 32 cm), which was filled with room temperature fresh tap water (25°C) to 1 cm below the surface of the platform (WAS), or kept empty (SHAM). The animals were exposed to this paradigm for 1 hour each day for 7 consecutive days, as described previously.^{6,7} The FPO of each animal was counted manually at the end of each session. The daily FPO and the average FPO of each animal through 7 days of WAS/SHAM was analyzed. On day 8, rats were subjected to colonic sensitivity assessment or tissue collection.

VMR to Tonic CRD

Colonic sensitivity was measured using a similar protocol as described previously.⁶ In brief, after an overnight fast, a 5-cm latex balloon (Trojan ENZ; Church & Dwight Co, Inc, Princeton, NJ), was inserted 11-cm into the proximal colon

under isoflurane anesthesia (2% inhalation, Isothesia; Henry Schein, Dublin, OH) and secured to the base of the tail with hypoallergenic silk tape. In freely moving rats, the number of abdominal contractions to colonic balloon distension was assessed visually to determine colonic sensitivity. The tonic CRD procedure consisted of series of constant pressure of 20, 40, or 60 mm Hg (10 min/distension, presented in a random order) with a 10-minute rest period (0 mm Hg) between distensions. The number of abdominal contractions was counted by an experimenter blinded to the treatment.

Stereotaxic Surgery and Minocycline/Fractalkine Infusion

Rats were anesthetized with isoflurane (2% inhalation). Cannulas (26-gauge; Plastics One, Roanoke, VA) were implanted with coordinates (from bregma -2.5 mm anterior-posterior, \pm 4.2 mm) medial-lateral, -7.0 mm dorsal-ventral, as previously described.⁶⁷ After recovering for 7 days from surgery, rats were infused with minocycline (10 μ g/ μ L, M9511; Sigma, St Louis, MO), fractalkine (20 ng/ μ L; R&D Systems, Minneapolis, MN) or vehicle (artificial cerebrospinal fluid) into CeA for 5 minutes (100 nL/min) under anesthesia (2% isoflurane inhalation). The concentration and infusion volume of minocycline and fractalkine were determined based on previously published studies.^{8,18,57,68} The rats were allowed to recover for 1 hour and then subjected to 1 hour of WAS or SHAM. This infusion/recovery/WAS (or SHAM) procedure was repeated for 7 consecutive days. On day 8, rats were subjected to colonic sensitivity assessment followed by death and tissue (brain) collection.

Immunofluorescence

Rats were anesthetized and perfused with phosphate-buffered saline (PBS) followed by 4% paraformaldehyde in PBS. The brain was collected and postfixed overnight in 4% paraformaldehyde at 4°C and cryoprotected with 30% sucrose solution in PBS. Nonconsecutive cryosections (8 μ m) were collected and stained with specific antibodies (Table 2). Secondary antibody only controls of immunofluorescence were conducted following the same protocol without primary antibodies and sections were imaged under the same microscopy settings as experimental sections from the same animal.

Image Analysis

Images for microglial morphology and phospho-p38 expression were captured with an AxioVert 200m Inverted Fluorescent microscope (Zeiss, Jena, Germany). For morphology, 3 z-stack images (21 slices per image, 6 μ m in total thickness) were taken for each animal from 3 noncontinuous sections. The microglial subtypes were analyzed by an investigator blinded to the treatment. The soma size and area occupied by microglial processes were measured using ImageJ/Fiji software (National Institutes of Health Bethesda, MD).^{24,69,70} For phospho-p38 expression, 3 single-stack images were taken from 3 noncontinuous sections of each animal. The quantification was presented as the volume% of phospho-p38-positive pixels in Iba-1-positive cells.

For GR localization and PSD-95-positive puncta in the microglia, z-stack images were acquired (14 slices, 6.15 μ m in total thickness) with a Zeiss LSM-710 confocal microscope under 63 \times objective in 2 \times zoom (GR expression) or 3 \times zoom (PSD95). For GR localization, 6–8 microglia from 3 noncontinuous sections were analyzed for each animal. Cytoplasmic and nuclear microglial GR expression was determined by Fiji as a ratio of GR-positive pixels in the cytoplasm (colocalized with Iba-1) vs GR-positive pixels in the nucleus (colocalized with 4',6-diamidino-2-phenylindole) in all z-stack slices. PSD-95-positive puncta in each microglia were counted through entire z-stacks of each image. Six to 10 microglia from 3 noncontinuous sections were analyzed for each animal. For both GR and PSD-95 expression, cells were chosen randomly from both the left and right CeA of each section. Slides were coded and the experimenter was blinded to the treatment.

Quantitation of Proinflammatory Cytokine mRNA Levels

On day 8, the CeA was isolated as described previously.⁵⁷ IL1 β (Rn00580432; Applied Biosystems, Foster City, CA), TNF α (Rn01525859; Applied Biosystems), and IL6 (Rn01410330; Applied Biosystems) mRNA expression level by real-time PCR using TaqMan Gene Expression Essay Master Mix (Applied Biosystems) with rat glyceraldehyde-3-phosphate dehydrogenase (cat. 4352338E; Applied Biosystems) as the internal reference gene. Fold change in mRNA expression was calculated using the 2(-Delta Delta C(T)) method.⁷¹

Table 2. List of Primary Antibodies

Antibody	Dilution	Host	Company	Research Resource Identifier
Iba1	1:300	Rabbit	Wako (Richmond, VA)	N/A
Phospho-p38	1:100	Mouse	Cell Signaling (Danvers, MA)	AB_331296
Phospho-p38	1:100	Rabbit	Cell Signaling	AB_331641
PSD95	1:100	Mouse	ThermoFisher (Waltham, MA)	AB_2092361
NeuN	1:200	Mouse	Millipore Sigma (Burlington, MA)	AB_2298772
GFAP	1:200	Mouse	Millipore Sigma	AB_11212597
GR	1:50	Mouse	Invitrogen (Carlsbad, CA)	AB_325427

GFAP, glial fibrillary acidic protein; NeuN, Neuronal Nuclei.

Luminex Analysis

In another cohort of animals, total protein was extracted from isolated CeA using the Bio-plex cell lysis kit (cat. 171304011; Bio-Rad, Hercules, CA). Total protein concentrations were determined with the Pierce BCA protein assay kit (cat. 23225; Thermo Fisher, Waltham, MA). The 23 cytokine levels were measured using the Bio-Plex Pro Rat Cytokine 23-Plex Assay kit (cat. 12005641; Bio-Rad) on the Bio-Plex 200 system (Bio-Rad) following the manufacturer's instructions.

Apoptosis Analysis

Cryosections (8 μm) from perfused brain tissue were used for apoptosis analysis following the protocol of the ApopTag Peroxidase *In Situ* Apoptosis Detection Kit (cat. S7100; Millipore Sigma, Darmstadt, Germany). Three nonconsecutive sections per animal were analyzed. Images were taken using a Zeiss AxioVert 200m inverted fluorescent microscope with a 20 \times objective.

Statistical Analysis

Statistical analysis was performed using GraphPad Prism version 8.0 (GraphPad Software, La Jolla, CA). All data were presented as the means \pm SD. Changes in response to colonic distension and microglia subtype ratios were analyzed by 2-way analysis of variance (ANOVA) followed by the Tukey multiple comparison post-test. Differences in daily FPO were determined by 2-way ANOVA with the Bonferroni post-test, whereas the average FPO, mRNA, and protein expression levels between the SHAM and WAS groups were determined by an unpaired Student *t* test. The significance of immunofluorescence data was detected by 1-way ANOVA (phospho-p38 and PSD95 expression) and 2-way ANOVA (GR expression) with the Bonferroni post-test. *P* values shown in the Results section represent the post hoc comparison between specific groups. A *P* value less than .05 was considered statistically significant.

All authors had access to the study data and reviewed and approved the final manuscript.

References

- Moloney RD, O'Mahony SM, Dinan TG, Cryan JF. Stress-induced visceral pain: toward animal models of irritable-bowel syndrome and associated comorbidities. *Front Psychiatry* 2015;6:15.
- Chey WD, Kurlander J, Eswaran S. Irritable bowel syndrome: a clinical review. *JAMA* 2015;313:949–958.
- Price JL. Comparative aspects of amygdala connectivity. *Ann N Y Acad Sci* 2003;985:50–58.
- Tillisch K, Mayer EA, Labus JS. Quantitative meta-analysis identifies brain regions activated during rectal distension in irritable bowel syndrome. *Gastroenterology* 2011;140:91–100.
- Wilder-Smith CH. The balancing act: endogenous modulation of pain in functional gastrointestinal disorders. *Gut* 2011;60:1589–1599.
- Myers B, Greenwood-Van Meerveld B. Differential involvement of amygdala corticosteroid receptors in visceral hyperalgesia following acute or repeated stress. *Am J Physiol Gastrointest Liver Physiol* 2012;302:G260–G266.
- Tran L, Chaloner A, Sawalha AH, Greenwood Van Meerveld B. Importance of epigenetic mechanisms in visceral pain induced by chronic water avoidance stress. *Psychoneuroendocrinology* 2013;38:898–906.
- Johnson AC, Tran L, Greenwood-Van Meerveld B. Knockdown of corticotropin-releasing factor in the central amygdala reverses persistent viscerosomatic hyperalgesia. *Transl Psychiatry* 2015;5:e517.
- Karperien A, Ahammer H, Jelinek HF. Quantitating the subtleties of microglial morphology with fractal analysis. *Front Cell Neurosci* 2013;7:3.
- Lehnardt S. Innate immunity and neuroinflammation in the CNS: the role of microglia in Toll-like receptor-mediated neuronal injury. *Glia* 2010;58:253–263.
- Wohleb ES, Franklin T, Iwata M, Duman RS. Integrating neuroimmune systems in the neurobiology of depression. *Nat Rev Neurosci* 2016;17:497–511.
- Bradesi S, Schwetz I, Ennes HS, Lamy CM, Ohning G, Fanselow M, Pothoulakis C, McRoberts JA, Mayer EA. Repeated exposure to water avoidance stress in rats: a new model for sustained visceral hyperalgesia. *Am J Physiol Gastrointest Liver Physiol* 2005;289:G42–G53.
- Hong S, Fan J, Kemmerer ES, Evans S, Li Y, Wiley JW. Reciprocal changes in vanilloid (TRPV1) and endocannabinoid (CB1) receptors contribute to visceral hyperalgesia in the water avoidance stressed rat. *Gut* 2009;58:202–210.
- Cheng JK, Ji RR. Intracellular signaling in primary sensory neurons and persistent pain. *Neurochem Res* 2008;33:1970–1978.
- Ji RR, Gereau RWt, Malcangio M, Strichartz GR. MAP kinase and pain. *Brain Res Rev* 2009;60:135–148.
- Svensson CI, Marsala M, Westerlund A, Calcutt NA, Campana WM, Freshwater JD, Catalano R, Feng Y, Protter AA, Scott B, Yaksh TL. Activation of p38 mitogen-activated protein kinase in spinal microglia is a critical link in inflammation-induced spinal pain processing. *J Neurochem* 2003;86:1534–1544.
- Lu C-L. Spinal microglia: a potential target in the treatment of chronic visceral pain. *J Chinese Med Assoc* 2014;77:3–9.
- Bradesi S, Svensson CI, Steinauer J, Pothoulakis C, Yaksh TL, Mayer EA. Role of spinal microglia in visceral hyperalgesia and NK1R up-regulation in a rat model of chronic stress. *Gastroenterology* 2009;136:1339–1348. e2.
- Maatouk L, Compagnion AC, Sauvage MC, Bemelmans AP, Leclere-Turbant S, Cirotteau V, Tohme M, Beke A, Trichet M, Bazin V, Trawick BN, Ransohoff RM, Tronche F, Manoury B, Vyas S. TLR9 activation via microglial glucocorticoid receptors contributes to degeneration of midbrain dopamine neurons. *Nat Commun* 2018;9:2450.

20. Chan TE, Grossman YS, Bloss EB, Janssen WG, Lou W, McEwen BS, Dumitriu D, Morrison JH. Cell-type specific changes in glial morphology and glucocorticoid expression during stress and aging in the medial prefrontal cortex. *Front Aging Neurosci* 2018;10:146.
21. Bouazza B, Debba-Pavard M, Amrani Y, Isaacs L, O'Connell D, Ahamed S, Formella D, Tliba O. Basal p38 mitogen-activated protein kinase regulates unliganded glucocorticoid receptor function in airway smooth muscle cells. *Am J Respir Cell Mol Biol* 2014;50:301–315.
22. Kettenmann H, Hanisch UK, Noda M, Verkhratsky A. Physiology of microglia. *Physiol Rev* 2011;91:461–553.
23. Torres-Platas SG, Comeau S, Rachalski A, Bo GD, Cruceanu C, Turecki G, Giros B, Mechawar N. Morphometric characterization of microglial phenotypes in human cerebral cortex. *J Neuroinflammation* 2014;11:12.
24. Preissler J, Grosche A, Lede V, Le Duc D, Krugel K, Matyash V, Szulzewsky F, Kallendrusch S, Immig K, Kettenmann H, Bechmann I, Schoneberg T, Schulz A. Altered microglial phagocytosis in GPR34-deficient mice. *Glia* 2015;63:206–215.
25. Myers B, Greenwood-Van Meerveld B. Corticosteroid receptor-mediated mechanisms in the amygdala regulate anxiety and colonic sensitivity. *Am J Physiol Gastrointest Liver Physiol* 2007;292:G1622–G1629.
26. Pariante CM, Pearce BD, Pisell TL, Owens MJ, Miller AH. Steroid-independent translocation of the glucocorticoid receptor by the antidepressant desipramine. *Mol Pharmacol* 1997;52:571–581.
27. Szatmary Z, Garabedian MJ, Vilcek J. Inhibition of glucocorticoid receptor-mediated transcriptional activation by p38 mitogen-activated protein (MAP) kinase. *J Biol Chem* 2004;279:43708–43715.
28. Hong S, Dissing-Olesen L, Stevens B. New insights on the role of microglia in synaptic pruning in health and disease. *Curr Opin Neurobiol* 2016;36:128–134.
29. Hanisch U-K. Microglia as a source and target of cytokines. *Glia* 2002;40:140–155.
30. Morimoto N, Shimazawa M, Yamashima T, Nagai H, Hara H. Minocycline inhibits oxidative stress and decreases in vitro and in vivo ischemic neuronal damage. *Brain Res* 2005;1044:8–15.
31. Tikka T, Usenius T, Tenhunen M, Keinanen R, Koistinaho J. Tetracycline derivatives and ceftriaxone, a cephalosporin antibiotic, protect neurons against apoptosis induced by ionizing radiation. *J Neurochem* 2001;78:1409–1414.
32. Alano CC, Kauppinen TM, Valls AV, Swanson RA. Minocycline inhibits poly(ADP-ribose) polymerase-1 at nanomolar concentrations. *Proc Natl Acad Sci U S A* 2006;103:9685–9690.
33. Johnson AC, Myers B, Lazovic J, Towner R, Greenwood-Van Meerveld B. Brain activation in response to visceral stimulation in rats with amygdala implants of corticosterone: an fMRI study. *PLoS One* 2010;5:e8573.
34. Saab CY, Wang J, Gu C, Garner KN, Al-Chaer ED. Microglia: a newly discovered role in visceral hypersensitivity? *Neuron Glia Biol* 2006;2:271–277.
35. Wang YL, Han QQ, Gong WQ, Pan DH, Wang LZ, Hu W, Yang M, Li B, Yu J, Liu Q. Microglial activation mediates chronic mild stress-induced depressive- and anxiety-like behavior in adult rats. *J Neuroinflammation* 2018;15:21.
36. Bollinger JL, Bergeon Burns CM, Wellman CL. Differential effects of stress on microglial cell activation in male and female medial prefrontal cortex. *Brain Behav Immun* 2016;52:88–97.
37. Hinwood M, Tynan RJ, Charnley JL, Beynon SB, Day TA, Walker FR. Chronic stress induced remodeling of the prefrontal cortex: structural re-organization of microglia and the inhibitory effect of minocycline. *Cereb Cortex* 2013;23:1784–1797.
38. Wilder-Smith CH, Schindler D, Lovblad K, Redmond SM, Nirkko A. Brain functional magnetic resonance imaging of rectal pain and activation of endogenous inhibitory mechanisms in irritable bowel syndrome patient subgroups and healthy controls. *Gut* 2004;53:1595–1601.
39. Tran L, Greenwood-Van Meerveld B. Altered expression of glucocorticoid receptor and corticotropin-releasing factor in the central amygdala in response to elevated corticosterone. *Behav Brain Res* 2012;234:380–385.
40. Myers B, Greenwood-Van Meerveld B. Divergent effects of amygdala glucocorticoid and mineralocorticoid receptors in the regulation of visceral and somatic pain. *Am J Physiol Gastrointest Liver Physiol* 2010;298:G295–G303.
41. Greenwood-Van Meerveld B, Gibson M, Gunter W, Shepard J, Foreman R, Myers D. Stereotaxic delivery of corticosterone to the amygdala modulates colonic sensitivity in rats. *Brain Res* 2001;893:135–142.
42. Myers DA, Gibson M, Schulkin J, Greenwood Van-Meerveld B. Corticosterone implants to the amygdala and type 1 CRH receptor regulation: effects on behavior and colonic sensitivity. *Behav Brain Res* 2005;161:39–44.
43. Tynan RJ, Naicker S, Hinwood M, Nalivaiko E, Buller KM, Pow DV, Day TA, Walker FR. Chronic stress alters the density and morphology of microglia in a subset of stress-responsive brain regions. *Brain Behav Immun* 2010;24:1058–1068.
44. Bachstetter AD, Rowe RK, Kaneko M, Goulding D, Lifshitz J, Van Eldik LJ. The p38alpha MAPK regulates microglial responsiveness to diffuse traumatic brain injury. *J Neurosci* 2013;33:6143–6153.
45. Wen YR, Suter MR, Ji RR, Yeh GC, Wu YS, Wang KC, Kohno T, Sun WZ, Wang CC. Activation of p38 mitogen-activated protein kinase in spinal microglia contributes to incision-induced mechanical allodynia. *Anesthesiology* 2009;110:155–165.
46. Ji RR, Suter MR. p38 MAPK, microglial signaling, and neuropathic pain. *Mol Pain* 2007;3:33.
47. Yu T, Zhang X, Shi H, Tian J, Sun L, Hu X, Cui W, Du D. P2Y12 regulates microglia activation and excitatory synaptic transmission in spinal lamina II neurons during neuropathic pain in rodents. *Cell Death Dis* 2019;10:165.
48. Li Y, Liu L, Barger SW, Griffin WS. Interleukin-1 mediates pathological effects of microglia on tau phosphorylation and on synaptophysin synthesis in cortical neurons through a p38-MAPK pathway. *J Neurosci* 2003;23:1605–1611.
49. Owolabi SA, Saab CY. Fractalkine and minocycline alter neuronal activity in the spinal cord dorsal horn. *FEBS Lett* 2006;580:4306–4310.

50. Dworak M, Stebbing M, Kompa AR, Rana I, Krum H, Badoer E. Attenuation of microglial and neuronal activation in the brain by ICV minocycline following myocardial infarction. *Auton Neurosci* 2014;185:43–50.
51. Lin S, Zhang Y, Dodel R, Farlow MR, Paul SM, Du Y. Minocycline blocks nitric oxide-induced neurotoxicity by inhibition p38 MAP kinase in rat cerebellar granule neurons. *Neurosci Lett* 2001;315:61–64.
52. Pi R, Li W, Lee NT, Chan HH, Pu Y, Chan LN, Sucher NJ, Chang DC, Li M, Han Y. Minocycline prevents glutamate-induced apoptosis of cerebellar granule neurons by differential regulation of p38 and Akt pathways. *J Neurochem* 2004;91:1219–1230.
53. Xavier AM, Anunciato AK, Rosenstock TR, Glezer I. Gene expression control by glucocorticoid receptors during innate immune responses. *Front Endocrinol (Lausanne)* 2016;7:31.
54. Madalena KM, Lerch JK. The effect of glucocorticoid and glucocorticoid receptor interactions on brain, spinal cord, and glial cell plasticity. *Neural Plast* 2017;2017:8640970.
55. van Olst L, Bielefeld P, Fitzsimons CP, de Vries HE, Schouten M. Glucocorticoid-mediated modulation of morphological changes associated with aging in microglia. *Aging Cell* 2018;17:e12790.
56. Horchar MJ, Wohleb ES. Glucocorticoid receptor antagonism prevents microglia-mediated neuronal remodeling and behavioral despair following chronic unpredictable stress. *Brain Behav Immun* 2019;81:329–340.
57. Johnson AC, Greenwood-Van Meerveld B. Knockdown of steroid receptors in the central nucleus of the amygdala induces heightened pain behaviors in the rat. *Neuropharmacology* 2015;93:116–123.
58. Pace TW, Miller AH. Cytokines and glucocorticoid receptor signaling. Relevance to major depression. *Ann N Y Acad Sci* 2009;1179:86–105.
59. Morris GP, Clark IA, Zinn R, Vissel B. Microglia: a new frontier for synaptic plasticity, learning and memory, and neurodegenerative disease research. *Neurobiol Learn Mem* 2013;105:40–53.
60. Sellgren CM, Gracias J, Watmuff B, Biag JD, Thanos JM, Whittredge PB, Fu T, Worringer K, Brown HE, Wang J, Kaykas A, Karmacharya R, Goold CP, Sheridan SD, Perlis RH. Increased synapse elimination by microglia in schizophrenia patient-derived models of synaptic pruning. *Nat Neurosci* 2019;22:374–385.
61. Paolicelli RC, Bolasco G, Pagani F, Maggi L, Scianni M, Panzanelli P, Giustetto M, Ferreira TA, Guiducci E, Dumas L, Ragozzino D, Gross CT. Synaptic pruning by microglia is necessary for normal brain development. *Science* 2011;333:1456–1458.
62. Sarn N, Jaini R, Thacker S, Lee H, Dutta R, Eng C. Cytoplasmic-predominant Pten increases microglial activation and synaptic pruning in a murine model with autism-like phenotype. *Mol Psychiatry* 2020. <https://doi.org/10.1038/s41380-020-0681-0>.
63. Trapp BD, Wujek JR, Criste GA, Jalabi W, Yin X, Kidd GJ, Stohlman S, Ransohoff R. Evidence for synaptic stripping by cortical microglia. *Glia* 2007;55:360–368.
64. Blandino P Jr, Barnum CJ, Deak T. The involvement of norepinephrine and microglia in hypothalamic and splenic IL-1 β responses to stress. *J Neuroimmunol* 2006;173:87–95.
65. Zhang G, Zhao BX, Hua R, Kang J, Shao BM, Carbonaro TM, Zhang YM. Hippocampal microglial activation and glucocorticoid receptor down-regulation precipitate visceral hypersensitivity induced by colorectal distension in rats. *Neuropharmacology* 2016;102:295–303.
66. Zhang G, Yu L, Chen ZY, Zhu JS, Hua R, Qin X, Cao JL, Zhang YM. Activation of corticotropin-releasing factor neurons and microglia in paraventricular nucleus precipitates visceral hypersensitivity induced by colorectal distension in rats. *Brain Behav Immun* 2016;55:93–104.
67. Johnson AC, Tran L, Schulkin J, Greenwood-Van Meerveld B. Importance of stress receptor-mediated mechanisms in the amygdala on visceral pain perception in an intrinsically anxious rat. *Neurogastroenterol Motil* 2012;24:479–486, e219.
68. Mendiola AS, Garza R, Cardona SM, Mythen SA, Lira SA, Akassoglou K, Cardona AE. Fractalkine signaling attenuates perivascular clustering of microglia and fibrinogen leakage during systemic inflammation in mouse models of diabetic retinopathy. *Front Cell Neurosci* 2016;10:303.
69. Fernandez-Arjona MDM, Grondona JM, Granados-Duran P, Fernandez-Llerez P, Lopez-Avalos MD. Microglia morphological categorization in a rat model of neuroinflammation by hierarchical cluster and principal components analysis. *Front Cell Neurosci* 2017;11:235.
70. Morrison H, Young K, Qureshi M, Rowe RK, Lifshitz J. Quantitative microglia analyses reveal diverse morphologic responses in the rat cortex after diffuse brain injury. *Sci Rep* 2017;7:13211.
71. Livak KJ, Schmittgen TD. Analysis of relative gene expression data using real-time quantitative PCR and the 2(-Delta Delta C(T)) Method. *Methods* 2001;25:402–408.

Received December 13, 2019. Accepted April 30, 2020.

Correspondence

Address correspondence to: Beverley Greenwood-Van Meerveld, PhD, O'Donoghue Building, Room 332, 1122 NE 13th Street, Oklahoma City, Oklahoma 73117. e-mail: beverley-greenwood@ouhsc.edu.

Credit Authorship Contributions

Tian Yuan (Conceptualization: Lead; Data curation: Lead; Formal analysis: Lead; Investigation: Lead; Methodology: Lead; Writing – original draft: Lead); Krishna Manohar (Data curation: Equal; Formal analysis: Equal; Investigation: Equal; Methodology: Equal; Writing – review & editing: Equal); Rocco Latorre (Data curation: Equal; Formal analysis: Equal; Investigation: Equal; Methodology: Equal; Writing – review & editing: Equal); Albert Oroco (Data curation: Equal; Formal analysis: Equal; Methodology: Equal; Writing – review & editing: Supporting); Beverley Greenwood-Van Meerveld (Conceptualization: Lead; Data curation: Equal; Funding acquisition: Lead; Investigation: Equal; Resources: Lead; Supervision: Lead; Writing – review & editing: Lead).

Conflicts of interest

This author discloses the following: the research in Beverley Greenwood-Van Meerveld's laboratory is supported, in part, by Ironwood Pharmaceuticals, EA Pharma Co. Ltd, and TEVA Pharmaceuticals. The remaining authors disclose no conflicts.

Funding

This work was supported by in-house funds (B.G.-V.M.) and in part by a pilot grant from the Oklahoma Center for Neuroscience (R.L.). Also supported by a Department of Veterans Affairs Senior Research Career Scientist award (11K6BX003610-01) (B.G.-V.M.).